Food Chemistry xxx (xxxx) xxx-xxx

Contents lists available at ScienceDirect

Food Chemistry

journal homepage: http://ees.elsevier.com

Gold nanoparticles modified graphene platforms for highly sensitive electrochemical detection of vitamin C in infant food and formulae

Francesca Bettazzi [a], Chiara Ingrosso [b,c], Patrick Severin Sfragano [a], Valentina Pifferi [d], Luigi Falciola [c,d], M. Lucia Curri [b,c,e], Ilaria Palchetti [a,c]

[a] Dipartimento di Chimica, Università degli Studi di Firenze, Via della Lastruccia 3, 50019 Sesto Fiorentino, Firenze, Italy
[b] CNR-IPCF Istituto per i Processi Chimico-Fisici, Sez. Bari, c/o Dip. Chimica Via Orabona 4, 70126 Bari, Italy
[c] INSTM, Via G. Giusti 9, 50121 Firenze, Italy
[d] Dipartimento di Chimica, Università degli Studi di Milano, Via Golgi 19, 20133 Milano, Italy
[e] Dipartimento di Chimica, Università degli Studi di Bari, Via Orabona 4, 70126 Bari, Italy

ARTICLE INFO

Keywords
Vitamin C
Ascorbic acid
Screening
Commercial fortified food and formulae
Quality control
Reduced graphene oxide
Colloidal Au nanoparticles
Electrochemical sensor

ABSTRACT

An easy and reliable method based on a novel electroanalytical nanostructured sensor has been developed to perform quantification of vitamin C in commercial and fortified cow-milk-based formulae and foods for infants and young children. The work is motivated by the need of a reliable analytical tool to be applied in quality control laboratories for the quantitative assessment of vitamin C where its rapid and cost-effective monitoring is essential.The *ad hoc* designed sensor, based on disposable Screen-Printed Carbon Electrodes modified with Au nanoparticles decorated Reduced Graphene Oxide flakes, exhibits a LOD of 0.088 mg L^{-1}. The low cost, easy sample preparation, fast response and high reproducibility (RSD ≈ 8%) of the proposed method highlight its suitability for usage in quality control laboratories for determining vitamin C in real complex food matrices, envisaging the application of the sensing platform in the determination of other compounds relevant in food chemistry and food manufacturing.

1. Introduction

Vitamin C is one of the most important water soluble vitamins and it refers to all compounds exhibiting equivalent biological activity to L-ascorbic acid (AA) including dehydroascorbic acid (DHAA), the oxidation product of AA, its isomers and esters (Spínola et al., 2014). Humans are unable to synthetize vitamin C, thus it has to be supplied by the diet, in particular by fresh fruits and vegetables. For breast-fed infants, the intake of vitamin C is from human milk and, hence, it depends on the vitamin C status of the mother. Scurvy has been observed in sixth months old infants fed by a diet consisting of cow's milk with no fruits and vegetables ((EFSA), 2014). Fortified formulae and fortified foods (*i.e.* fortified cow's milk, fortified cereal-based foods and supplements) are means to increase vitamins, minerals and other nutrients intake in infants and young children with inadequate or at risk of inadequate status of these nutrients. Food and formulae for infants, aged from 0 to 1 year, and young children, from 1 to 3 years, must satisfy nutritional requirements in order to ensure a normal growth development and a good health status (Lermo et al., 2009; Silva et al., 2018). The European Food Safety Authority (EFSA) suggests a vitamin C daily intake of 20 mg for infants and young children ((EFSA), 2014; EFSA Panel on Dietetic Products, 2013). The U.S. National Academy of Science establishes as adequate intake of vitamin C 40 mg/day and 50 mg/day, for healthy infants aged between 0 and 6 months and 6 months to 1 year, respectively (National Academies of Sciences Engineering Medicine, n.d.). Vitamin C can be added to foods as AA, sodium L-ascorbate, calcium L-ascorbate, potassium ascorbate and 6-palmitoyl-L-ascorbic acid (ascorbyl palmitate) (European commission, 2006; Silva et al., 2018).

Concerns on the nutritional quality of vitamin C content in foods arise among both consumers and manufactures considering the possible vitamin losses during food process and storage. In fact, AA is rapidly oxidized to DHAA, being such an oxidation process induced by exposure to high temperatures and pH, light, presence of oxygen and other oxidants or metals. To address this issue, during food manufacturing a higher amount of vitamin C can be added to prevent its overestimation in the final product, and efficient control protocols are required to assess the compliance of vitamin C content to the nutrition label. Therefore, special emphasis has to be put to the development of a convenient and reliable analytical method, along with the setup of simple and reliable sample preparation procedures that take into account the high heterogeneity of the food formulae.

E-mail address: ilaria.palchetti@unifi.it (I. Palchetti)

https://doi.org/10.1016/j.foodchem.2020.128692
Received 13 June 2020; Received in revised form 29 October 2020; Accepted 18 November 2020
Available online xxx
0308-8146/

Different methods have been proposed for AA determination (Chebrolu, Jayaprakasha, Yoo, Jifon, & Patil, 2012; da Silva, Aguiar-Oliveira, Mazalli, Kamimura, & Maldonado, 2017; Gazdik et al., 2008; Mazurek & Jamroz, 2015)(). Among these, analysis based on High Performance Liquid Chromatography (HPLC) coupled to spectrophotometric detection has the advantage to be a reliable and robust reference method (Spínola et al., 2014). Enzymatic methods are also used with commercial test kits for AA levels spectrophotometric determination (Romeu-Nadal et al., 2006). Electrochemical detection is an attractive alternative approach for the detection of electroactive species, such as AA, in food matrix, because of the inherent advantages of simplicity, ease of miniaturization, high sensitivity and relatively low cost (Kizek, 2008; Bettazzi et al., 2006).

Although AA is an electroactive molecule, easy to be oxidized, and, therefore, electrochemically detectable, it forms with DHAA an irreversible redox couple. To catalyze the electrochemical oxidation of AA, many modified electrodes with an improved selectivity and sensitivity towards AA determination, have been proposed (Pisoschi et al., 2014; Falat & Cheng, 1983; Bettazzi et al., 2018).

So far, a number of hybrid nanocomposite materials have been developed as electrochemical sensors and biosensors for AA determination (Pisoschi et al., 2014). In particular, Reduced Graphene Oxide (RGO) is a well-known sp^2 hybridized planar carbon nanostructured material with interesting structural and superior conducting properties (Bonanni et al., 2012). RGO is considered a robust scaffold for manufacturing original and highly functional hybrid materials with Au nanoparticles (NPs) (Tiwari et al., 2015; Ingrosso et al., 2017). Au NPs decorated RGO sheets provide a very large electrochemically active surface area, leading to fast heterogeneous electron transfer kinetics and high electrocatalytic activity (Turcheniuk et al., 2015; Tiwari et al., 2015). Recently, Zhu et al. have proposed a three-dimensional graphene hydrogel and Au NPs nanocomposite (3DGH-AuNPs) for simultaneous detection of AA, dopamine (DA) and uric acid (UA), with a LOD for AA of 28 nM (Zhu et al., 2017). A glassy carbon electrode (GCE) modified with a 3D-networked nanostructure composed of MoS_2, RGO and Au NPs (3D-MoS_2/RGO/Au) has been developed for determination of AA with a LOD of 0.93 μM (Zhao et al., 2019). Ghambari et al have proposed RGO/polypyrrole (PPy)/Zinc Oxide (ZnO)/Au NPs nanocomposite modified GCEs for simultaneous determination of AA, epinephrine (EP) and uric acid (UA), with a linear response of 2–950 μM and LOD of 0.16 μM (Ghanbari & Hajian, 2017). A one-pot synthesis of Au NPs onto graphene, by *in situ* thermal reduction of hydrogen tetra-chloroaurate(III) ($HAuCl_4$) onto GO with β - cyclodextrin in alkaline condition, has been proposed for AA determination, obtaining a LOD of 10 μM and a linear response of 30–2000 μM (Tian et al., 2012). Au nanoplates and RGO modified GCEs have been fabricated *via* a simple electrochemical method for the determination of AA with a LOD of 51 μM (Wang et al., 2014).

Here, a novel electroanalytical approach has been implemented for highly sensitive determination of vitamin C in complex matrices. Disposable Screen-Printed Carbon Electrodes (SPCEs) have been modified by a hybrid nanocomposite recently developed by the authors' group, and formed of RGO flakes surface functionalized by 1-pyrene carboxylic acid (PCA), and *in situ* decorated by colloidal Au NPs (; Ingrosso et al., 2019). This novel nanocomposite has shown a low LOD in the biomolecules detection, that has been explained on the basis of a fast heterogeneous electron transfer (ET) kinetics and an increase of the electroactive surface area, along with an overall enhancement of the electrocatalytic properties towards diverse tested compounds (Ingrosso et al., 2019).

The aim of this work is to demonstrate that the proposed novel nanostructured electroanalytical platform enables a reliable and rapid vitamin C monitoring in complex commercial cow-milk-based formulae and food for infants and young children without any time consuming pre-treatment of the samples, and with a LOD lower than other state of art graphene/Au NPs based electrode modifiers, and lower than that of a routine enzymatic spectrophotometric method. The applicability of the sensor platform in determining the total vitamin C content, given by the total contribution of AA and DHAA, has been also preliminarily assessed by implementing a procedure suited to convert the electrochemically inert DHAA in the electroactive form AA, by a sample treatment with tris[2-*carboxyethyl*]phosphine hydrochloride (TCEP).

2. Materials and methods

2.1. Materials

Commercial RGO (1.6 nm thick flakes) was purchased from Graphene Supermarket. 1-pyrenecarboxylic acid (PCA, 97%), *n*-methyl-2-pyrrolidone (NMP, 99%), tetraoctylammonium bromide (TOAB, 99%), hydrogen tetrachloroaurate(III) trihydrate ($HAuCl_4{\cdot}3H_2O$, 99.999%), 3,4–dimethylbenzenethiol (DMBT, 98%), sodium borohydride ($NaBH_4$, 99.99%), toluene, methanol, L-ascorbic acid (AA), tris[2-*carboxyethyl*]phosphine hydrochloride (TCEP) and di-sodium hydrogen phosphate dodecahydrate, were purchased from Sigma (Milano, Italy). Potassium chloride, potassium dihydrogenphosphate and other chemicals were acquired from Merck (Milano, Italy).

Water from Milli-Q Water Purification System (Millipore, UK) was used for the preparation of all aqueous solutions.

The measurements were performed in 100 mM phosphate solutions (0.064 M $Na_2HPO_4{\cdot}2H_2O$ and 0.036 M $NaH_2PO_4{\cdot}H_2O$) containing 100 mM KCl at different pH (PS-phosphate saline-solution).

Pasteurized, cow's milk (1.6% fat content) formulae and food for infants from different producers were purchased from local stores.

2.2. Characterization techniques

All electrochemical measurements were performed with a μAUTOLAB type III digital potentiostat/galvanostat, controlled by the GPES 4.9004 software (Eco Chemie BV, Utrecht, The Netherlands).

The Screen-Printed Carbon Electrodes (SPCEs), consisting of a carbon working electrode (3 mm diameter), a carbon counter and a silver pseudo-reference electrode, were obtained by Ecobioservices and Researches (EBSR, Firenze, Italy). SPCEs were used as received, without any preliminary cleaning treatment (Bettazzi et al., 2013; Laschi et al., 2006). Amperometric measurements were performed in an electrolytic solution of 5 mL, and a magnetic stirrer was used to ensure convective mass transport in the solution during the amperometric experiments.

The enzymatic AA colorimetric kit (cat.n. 10409677035) was obtained from R-Biopharm Italia Srl (Milano, Italy) and used according to the indications of the manufacturer. A LOD of 0.3 mg L^{-1} is reported in the manufacturer's instruction.

The UV–Vis spectrophotometer EVOLUTION220 (Thermo Scientific) controlled by Thermo Insight software, equipped with the ECOLINE RE112 thermostatic water-bath, was used for the spectrophotometric analysis of the samples.

Transmission Electron Microscopy (TEM) images were recorded by using a Jeol Jem-1011 microscope operating at 100 kV, equipped with a high-contrast objective lens, a W filament as electron source, and having an ultimate point resolution of 0.34 nm. Images were acquired by a Quemesa Olympus CCD 11 Mp Camera. Samples were prepared by dipping a 300-mesh amorphous carbon-coated Cu grid in toluene solutions of the Au NPs/PCA-RGO hybrid nanocomposites, and leaving the solvent to evaporate. Statistical size analysis of the

NPs average size and size distribution was performed by using the freeware ImageJ analysis program.

Field Emission Scanning Electron Microscopy (FE-SEM) was performed by a Zeiss Sigma microscope operating in the range of 0–10 kV, and equipped with both an in-lens secondary electron detector, and an INCA Energy Dispersive Spectroscopy (EDS) detector. Samples were mounted onto stainless-steel sample holders by a double-sided conductive carbon tape and grounded by silver paste.

Mid-infrared spectra were acquired with a Varian 670-IR spectrometer equipped with a DTGS (deuterated triglycine sulfate) detector. The spectral resolution used for all experiments was 4 cm^{-1}. For attenuated total reflection (ATR) measurements, a one-bounce 2 mm diameter diamond microprism was used as the internal reflection element (IRE). Films were directly cast onto the internal reflection element by depositing the solution onto the upper face of the diamond crystal and allowing the solvent to evaporate.

2.3. Synthesis of the Au NPs/PCA-RGO hybrid nanocomposite

The hybrid nanocomposite was synthesized as reported in (Ingrosso et al., 2019). Briefly, commercial RGO was exfoliated and functionalized with PCA, by stirring and sonicating a mixture of PCA and RGO prepared with a 17:1 w/w ratio in NMP. The excess of PCA was removed by cycles of centrifugation and re-dispersion in methanol, and the purified PCA-RGO complex was re-dispersed in NMP (Ingrosso et al., 2019). The Au NPs/PCA-RGO hybrid material was obtained by suitably modifying the two-phase colloidal method of Brust et al. (Ingrosso et al., 2019) . In a typical experiment, 15 mg of the PCA modified RGO powder (PCA-RGO) were dissolved in a solution prepared by mixing 1.1872 g of TOAB in 35 mL of toluene, and left to stir 30 min. To this solution, 0.1770 g of $HAuCl_4{\cdot}3H_2O$ dispersed in 15 mL of MilliQ water, were added and left to stir 30 min. After transfer of the Au precursor from water to toluene, which is assisted by TOAB, water was removed from the reaction flask, and 120 μL of DMBT were added for allowing controlled reduction of Au(III) to Au(I), and left to stir 1 h. Finally, 0.1892 g of $NaBH_4$ in 12 mL of MilliQ water were added, and the growth of the Au NPs was allowed to proceed overnight. The Au NPs/PCA-RGO dispersions were then purified with methanol by cycles of centrifugation to remove the excess of DMBT. Finally, homonucleated Au NPs were separated from the Au NPs/PCA-RGO hybrid flakes, by means of a precipitation procedure (Ingrosso et al., 2019).

2.4. Electrochemical measurements

Cyclic voltammetry (CV) experiments were performed by exposing the SPCEs, modified by drop-casting 1 μL of the Au NPs/PCA-RGO dispersion, to 70 μL of the AA solution (1 mM AA in PS solution at different pH), and by cycling the potential linearly, in the range −0.10 - +0.7 V vs. Ag/AgCl, with a scan rate of 50 mV s^{-1}. Hydrodynamic voltammetry measurements were performed in 5 mL of treated skimmed-milk sample, spiked with 500 μM AA, at pH 3.5, by applying a fixed potential in the range of 0 - +0.4 V vs. Ag/AgCl, under stirring. Amperometric measurements were performed by applying a fixed potential of +0.1 V in 5 mL of PS solution (pH 3.5) or by applying a fixed potential of +0.3 V in treated milk samples (pH 3.5). The calibration curve was performed under stirring conditions, by adding AA at different concentrations. All potentials were referred to the screen-printed silver pseudo-reference electrode and the experiments were carried out at room temperature.

AA stock solution was prepared fresh in amber vial at the beginning of each experimental session and stored in an ice-bath-equipment (closed with a cap to avoid light) between measurements.

2.5. Sample preparation

Commercial milk formulae and food by different producers were purchased from local stores. The calibration curve in matrix was performed by using a commercial, pasteurized and skimmed cow's milk.

Aliquots of pasteurized cow's milk (1.6% fat content) and liquid commercial milk formulae were treated by addition of 500 μL of 10 M HCl to 50 mL of sample, in order to achieve protein precipitation (de-proteinization). The resulting pH of the sample is around 3.5. Mixtures were then centrifuged at 8000 g for 10 min; the obtained liquid phase was thus collected and analyzed. Solid samples were dispersed in 50 mL of PS solution at pH 3.5 and centrifuged. The liquid phase was collected and analyzed. The use of HCl allows the achievement of a constant value of chloride ion concentration useful for electrochemical measurements.

Spectrophotometric measurements of the samples were performed following the manufacturer instruction.

When TCEP is used, 5 mL of a milk sample, with a declared amount of vitamin C of 10 mg/100 mL, were added by TCEP to a final concentration of 500 μM, and the TCEP reduction reaction was allowed to proceed for 1 h. Then, the milk sample was added by 50 μL of 10 M HCl solution for de-proteinization, and successively centrifuged for 10 min.

2.6. Calibration plot and statistical analysis of samples

The calibration plot was fitted to a linear model function (y = ax + b) by weighted linear least-squares method, by using Origin Pro 2019b software (Origin Lab Corporation, USA) and $w = 1/\sigma_i^2$ as weight.

The limit of detection (LOD) was calculated according to the equation:

$$LOD = 3.3\left(s_{y/x}/S\right)$$

where $s_{y/x}$ is the residual standard deviation and S is the slope of the calibration plot (calibration sensitivity) (Brunetti & Desimoni, 2014). The following equation was used for the limit of quantification (LOQ) evaluation:

$$LOQ = 10\left(s_{y/x}/S\right)$$

The content of AA in real samples was evaluated by the standard addition method (sample + three additions). All the reported results are mean values obtained analyzing three individual portions of the same sample. The results obtained with the proposed procedure and by using the Au NPs/PCA-RGO modified SPCEs (AuNPs/RGO/SPCEs) were compared with those obtained by the routine enzymatic spectrophotometric method, by analyzing samples at variable analyte concentration and at different composition. A linear regression analysis was performed by using the "errors-in-variables regression methods", that is by considering errors in both variables (X,Y) and by using the routine method results (spectrophotometric) as standard (X).

To test for bias, *i.e.* the equivalence of the compared methods, the 95%-confidence intervals of the estimators from the linear equations, y = ax + b, obtained after the orthogonal regression, were used to test whether the optimal estimators of a = 1 and b = 0 are included in the spanned confidence intervals. The software Origin Pro 2019b, linear fit with X error, following the York computation method was used, correlation between X and Y errors = 0. Pearson correlation at the 5% level of significance (95% confidence level) was also evaluated. Results are reported at first significant figure of their uncertainty.

3. Results and discussion

Disposable Screen Printed Electrodes (SPCEs) have been modified by a recently developed novel hybrid nanocomposite, based on RGO flakes surface functionalized by 1-pyrenecarboxyl acid (PCA) and decorated by colloidal Au NPs (Au NPs/PCA-RGO), *in situ* synthesized onto the oxygen based functionalities of the PCA-RGO complex (Goncalves et al., 2009). The short aromatic thiol 3,4–dimethylbenzenethiol (DMBT) reduces the $HAuCl_4{\cdot}3H_2O$ precursor to Au(I), which then goes to Au(0) by $NaBH_4$ addition, and it functions as capping ligand, controlling NPs morphology and size dispersion (Ingrosso et al., 2019). In addition, it further promotes NPs anchoring onto the flakes by π-π interactions and enables NPs/RGO electronic coupling, finally providing the hybrid structure with a high conductivity (Ingrosso et al., 2019).

The Au NPs/PCA-RGO hybrid nanocomposite presents the morphology observed in the TEM image of Fig. S1A that shows RGO flakes densely coated by spherical high contrast nanostructures reasonably ascribed to the Au NPs.

The coordination of the DMBT thiol to the surface of the Au NPs, assessed by the Attenuated total reflection Fourier-transform infrared (ATR-FTIR) spectra of Fig. S1B, explains the dispersibility of the hybrid nanocomposite in organic solvents, and grants its processability from solution, hence resulting effective for further investigation and final integration in devices for applications (Chiara Ingrosso et al., 2019).

The SEM image of Fig. 1A shows the typical surface morphology of the Au NPs/PCA-RGO hybrid nanocomposite deposited by drop-casting onto SPCEs. As it can be noticed, it resembles that of the Au NPs/PCA-RGO hybrid sample deposited onto silicon (Fig. S1C), showing corrugations, bright contrast wrinkles and folded edges typical of the PCA-RGO sheets (Ingrosso et al., 2019), along with bright contrast nanostructures compatible with the Au NPs.

3.1. Electrochemical investigation of AA

The electrochemical performance of the Au NPs/PCA-RGO modified SPCEs (AuNPs/RGO/SPCEs) has been investigated by collecting CVs in 0.1 M PS solution (pH 3.5) in absence and in presence of AA. The CV responses of (a) bare and (b) AuNPs/RGO/SPCEs towards the detection of 1 mM AA in 0.1 M PS (pH 3.5) at a scan rate of 50 mV s^{-1}, have been collected keeping constant the geometrical area of the working electrode (7 mm^2) (Fig. 1B). The peak observed at both the electrodes is assigned to the electrochemical oxidation of AA to dehydroascorbic acid (DHAA). The AuNPs/RGO/SPCEs exhibit a higher peak current and a potential negatively shifted of $\cong$ 120 mV (E_{ap} = 244 mV) with respect to the bare SPCEs (Fig. 1C). During the reverse scan, no cathodic peak is observed for AA, pointing out the expected irreversibility of this oxidation process. The AuNPs/RGO/SPCE clearly favors the AA oxidation, as evident from the decrease of the overpotential, when compared to the bare SPCE. This advantage could be due to an electrocatalytic effect of the composite material and a thin-layer effect brought by the porous layer of RGO (Compton & Banks, 2010). The effect of the scan rate (10–100 mV s^{-1}) has been investigated towards the oxidation of AA, as shown in Fig. 1C. Increasing the scan rates (from 10 to 100 mV s^{-1}), the oxidation peak potential has been found to shift towards more anodic values, indicating the kinetic limitation of the electron transfer reaction. The proportional linear relationship of the logarithm of the scan rate (log ν) vs. the anodic peak potential (E_{ap}) with a slope greater than 30 mV per decade, reported in Fig. 1D, confirms the irreversibility of the redox process (Nicholson & Shain, 1964; Klingler & Kochi, 1980). Fig. 1D shows also the linear relationship between the square root of the scan rate and the peak current (I_{ap}) of AA. The peak currents can be fitted by linear re-

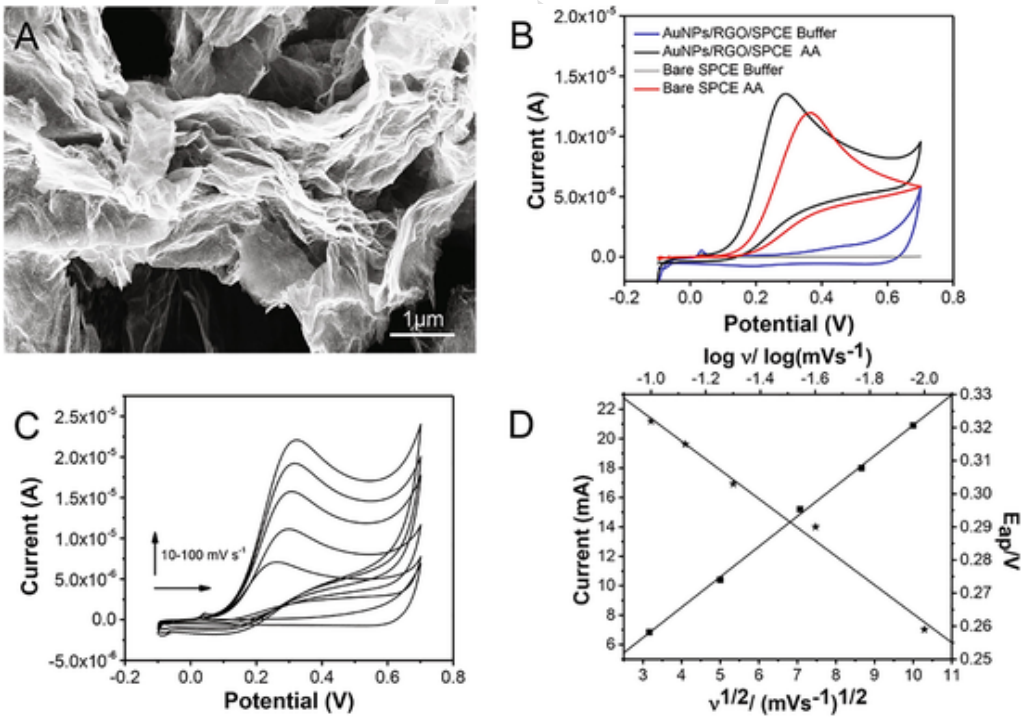

Fig. 1. A) SEM image of Au NPs/RGO/SPCEs (42.93 KX). B) CVs recorded at the AuNPs/RGO/SPCEs and bare SPCEs in 100 mM PS at pH 3.5, as neat and added by 1 mM AA, in the −0.10 – +0.70 V potential range and scan rate of 50 mV s^{-1}. C) CVs recorded from −0.10 to + 0.70 V, at different scan rate, in 100 mM PS at pH 3.5. D) Plot of i_{ap} of B vs. $\nu^{1/2}$ and plot of E_{ap} of AA vs. log ν.

gression with a correlation coefficient of 0.998, which suggests a diffusion-controlled electron transfer process.

The oxidation at different pH has been also studied by CV experiments over the potential range from −0.1 V to +0.8 V (Fig. S2). In the 3.5 to 6 pH range the oxidation peak potential moves to lower values at increasing solution pH. It is known that at a pH lower than the first pK_a of AA (approximately 4.5), two protons interchange globally during the process (Rueda et al., 1978). At pH values higher than the pK_a, a single proton interchanges, with ascorbate anion as electroactive species. These considerations are consistent with the dependence of the peak potential on the pH. A higher oxidation peak current is observed at pH 3.5, while increasing the solution pH the peak current gradually decreases and the peak potential shifts towards more negative values. Furthermore, AA is stable in acidic media. Hence, the pH 3.5 has been chosen thereon as optimum condition for further characterizing the AuNPs/RGO/SPCEs in the electrooxidation of AA.

3.2. Calibration procedure

Calibration curve of AA in 0.1 M PS (pH 3.5) has been obtained for both the bare and modified SPCEs. Amperometric measurements of AA at the constant applied potential of +0.10 V, in a magnetically stirred solution at pH 3.5, have been carried out, and the current response is extremely rapid, achieving steady-state current in less than 5 s (inset in Fig. 2A). Preliminary experiments (Fig. S3) have demonstrated that at this potential the current at the hybrid modified SPCE is almost 100-fold higher than at the bare SPCE. The current response obtained measuring AA standard solutions (Fig. 2B), shows a linear relationship over the investigated concentration range (y = (2.25 ± 0.07)x + 1.48 ± 0.38), with a correlation coefficient of r^2 = 0.990. From the analysis of the data obtained from the calibration curve, the estimated LOD of AA is 0.5 μM (0.088 mg L^{-1}) and the LOQ is 1.5 μM for the AuNPs/RGO/SPCE. As expected, both the LOD and the LOQ obtained at the bare electrode are higher than those at the AuNPs/RGO/SPCE (Fig. 2).

Remarkably, the LOD value estimated by using the proposed nanostructured platforms (0.5 μM) has been found lower than other LOD values recently reported for systems based on graphene/AuNPs nanocomposites modified electrodes, including 3D-MoS_2/RGO/Au (Zhao et al., 2019), Au NP/RGO (Tian et al., 2012), and others systems (Table S1).

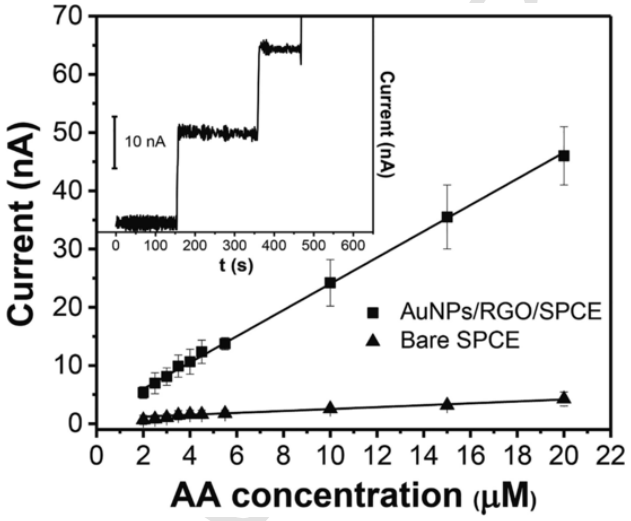

Fig. 2. (A) Calibration plot of AA in 100 mM PS (pH 3.5) at AuNPs/RGO/SPCEs (■) and bare SPCEs (▲). The error bars correspond to the standard deviation (n = 3). Constant applied potential of + 0.10 V vs. Ag/AgCl. (B) Amperometric response upon AA addition at the AuNPs/RGO/SPCEs.

3.3. Analysis of AA in commercial infant foods and formulae

In the analysis of real samples, the analytical parameters of the method, including LOD, LOQ, and precision are expected to be affected by the presence of matrix components, possibly causing inaccuracy in the results. Therefore, a calibration curve has been built by spiking cow's milk samples with a known amount of AA. To this end, known volumes of HCl have been added to weighted amounts of low-fat, cow's milk samples that have been then centrifuged and decanted. The achieved liquid phase has been collected and analyzed, and the results have been reported as mean values obtained analyzing three distinct aliquots of the same sample.

At first, an amperometric hydrodynamic voltammetry of AA, in the range of −0.1 V – +0.4 V, has been carried out in order to evaluate the effect of the applied potential on the oxidation of 500 μM of AA, in milk samples (pH 3.5), and to identify the most suited working potential. A comparison of the current values obtained for the modified and bare SPCEs, respectively, shows that the currents recorded at the AuNPs/RGO/SPCEs are higher than those of unmodified SPCEs over the whole investigated potential range. At +0.3 V the current is ca. two orders of magnitude higher than those obtained at the bare SPCEs (Fig. 3 A). This enhanced response can be explained considering the increased active area of the AuNPs/RGO/SPCE nanostructured surface, due to the Au NPs nano-spacer behavior between the PCA–RGO sheets (Fig. 3C), and the higher electroactivity of the AuNPs/PCA-RGO hybrid. Thus, the AuNPs/RGO/SPCEs have then been proved efficient sensors for accomplishing a sensitive electrochemical determination of AA in complex matrix samples. In order to maximize the current response, a working potential of +0.3 V has been selected for the following experiments in real samples.

From the analysis of the data obtained from the calibration curve in milk samples, the estimated LOD of AA was 17 μM and 57 μM the LOQ (Fig. 3B).

The precision has been evaluated by repeating the measure of the current by using the AuNPs/PCA-RGO/SPCE electrode for each measurement (*i.e.* under repeatability condition). Concentration levels of 50 μM (70 ± 6nA) and 500 μM (600 ± 50nA) have been tested with %RSD of 8.6 and 8.3%, respectively (n = 5).

The large range of linearity (50–500 μM), and the estimated LOD and LOQ, well below the concentration of vitamin C generally found in commercial food products, demonstrate that the proposed AuNPs/RGO/SPCE sensors are definitely suitable for the investigation of AA in real food samples.

The electrochemical analysis of infant formulae and fortified milk-based food is challenged by the presence of many other vitamins, minerals and nutrients, some of them with redox properties. In particular, vitamins, both lipid soluble vitamins (A, D, E, and K) and water soluble vitamins (*i.e.* B vitamins), are generally present in formulae and food for infant and young children (Liu et al., 2016; Llorent-Martínez et al., 2006; Brunetti & Desimoni, 2014; Puangjan et al., 2017), therefore, their possible influence on the determination needs to be assessed. For this purpose, a vitamin mix formed of 3.8 μM vitamin B1 (thiamine), 4.5 μM vitamin B2 (riboflavin), 7.0 μM of vitamin B6 (pyridoxine), 100 μM of vitamin B8 (biotin) and 500 μM of vitamin B9 (folic acid), has been used as matrix for the amperometric measurements of AA at the AuNPs/RGO/SPCE, at the potential of +0.3 V. The results show that such a mix has only a slight effect on the AA determination (Fig. 4A).

Among the different nutrients, Fe(II) is generally added along with AA in infant formulae, since its absorption is facilitated by AA.

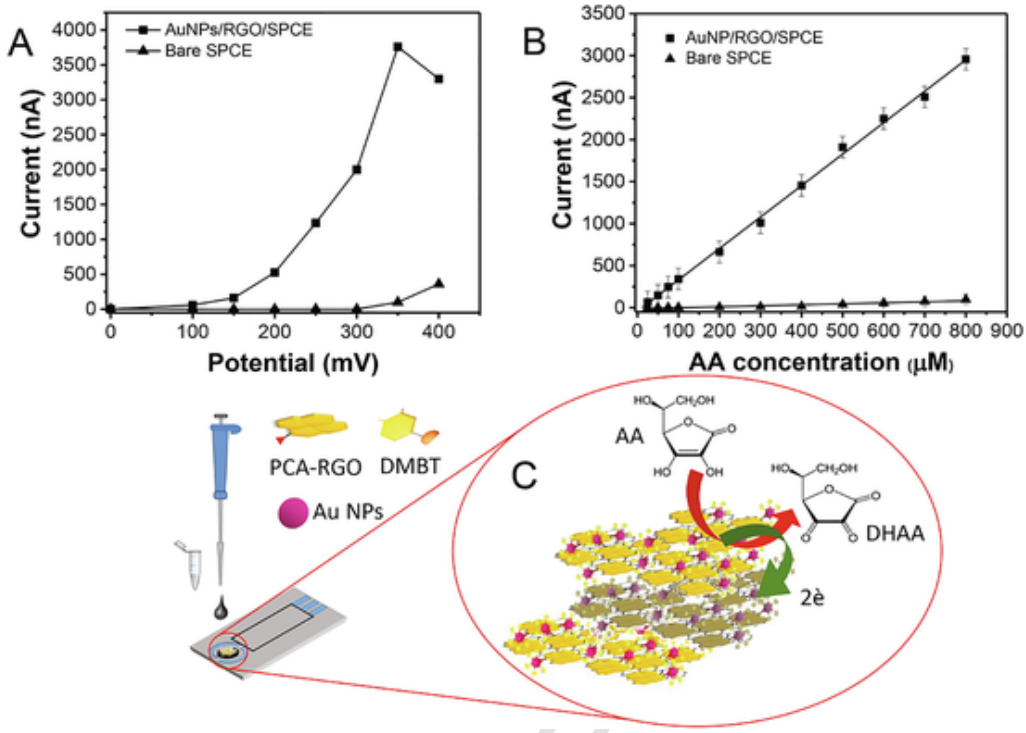

Fig. 3. A) Amperometric hydrodynamic voltammetry of 500 μM of AA in treated milk samples (pH 3.5), in the range 0 V – +0.4 V at AuNPs/RGO/SPCEs (■) and bare SPCEs (▲). B) Calibration plot of AA in treated milk samples at AuNPs/RGO/SPCEs (■) and bare SPCEs (▲). The error bars correspond to the standard deviation (n = 3). Constant applied potential of + 0.30 V vs. Ag/AgCl. C) Sketch of the AuNPs/RGO/SPCEs modified nanostructured platform and its application for AA determination in milk. (The schemes do not show properly the proportions of the reported structures).

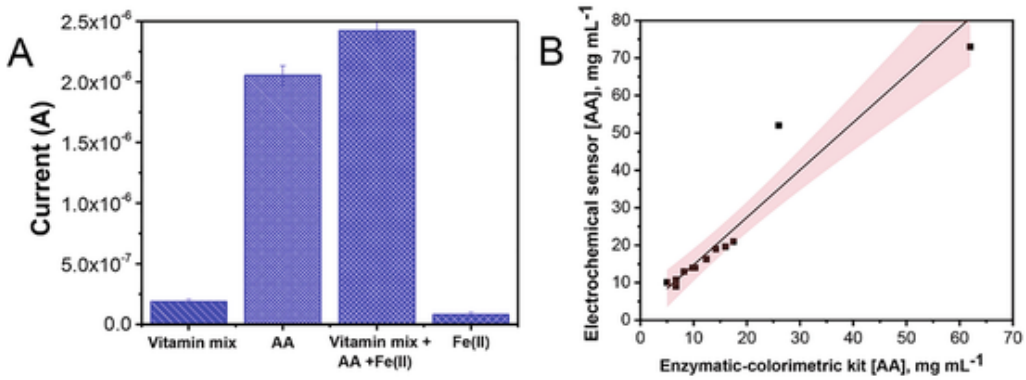

Fig. 4. A) Plot reporting the amperometric response at the AuNPs/RGO/SPCEs to the vitamin mix (3.8 μM vitamin B1, 4.5 μM vitamin B2, 7.0 μM vitamin B6, 100 μM vitamin B8, and 500 μM of vitamin B9), AA (600 μM) and Fe(II) (200 μM) compared to the mixture formed of vitamin mix, AA and Fe (II). B) Regression graph exhibiting the correlation of the two analytical methods with related confidence interval (95% confidence level).

The tested concentration of Fe(II) (200 μM) causes a negligible current signal in comparison to the oxidation current of AA.

It is worthwhile to point out that uric acid, also present may result an interferent in AA detection (Chen et al., 2002). However, CV recorded from a PS solution containing 0.1 mM uric acid by using the hybrid modified electrode (Fig. S4 of Supporting Information) points out that its oxidation peak is at +538 mV, a potential value higher than that of AA oxidation peak. The combination of such features, as the different oxidation potentials of the two compounds, the concentration of uric acid in infant formulae much lower than that of AA, and the use of the standard addition method to determine AA, generally able to mitigate interferent and matrix effects, all together, significantly reduces the interfering effect of uric acid in the proposed AA detection system.

3.4. Analysis of real samples

To assess the performance, and validate the proposed nanostructured sensing platform, a selected set of samples has been analyzed, and the results have been compared to those obtained by using a commercially available enzymatic kit, routinely used for spectrophotometric detection in quality control laboratories (Danielczuk et al., 2004). All the following experiments have been performed by the standard addition method, and the results have been reported as mean values obtained analyzing three single aliquots of the same sample.

In Fig. 4B the analysis of the regression function of the results, obtained in the two sets of experiments, is reported. The confidence

intervals include the optimal estimators for the slope and the intercept, which are one and zero, respectively, showing good agreement between the methods. The calculated Pearson correlation at the 5% level of significance is found to be r = 0.956 (n = 12), thus, confirming a good agreement. For each sample, the comparison between the two methods has been performed on the same day. A fresh AuNPs/RGO/SPCE has been used per sample.

The outlier point, observed out of the interval confidence (Fig. 4B), which highlights a significant discrepancy between the two methods can be explained considering that for the corresponding sample, the matrix is also formed of solid fruit and cereals, hence significantly different from the matrix of the other samples. Therefore, such a sample can be reasonably assumed to contain a different set of interfering compounds. Further experiments are thus needed to adapt sample treatment procedures to such a class of matrix.

Here, only the AA content has been taken into account and determined in each investigated food product, since in these types of products, vitamin C is typically added as sodium ascorbate. Nevertheless, in certain cases the determination of the content of DHAA, that is the AA oxidation product, can be relevant. Indeed, the sum of AA and DHAA amount in food has been proposed to be used as index of the health-related quality of food (Nováková et al., 2008), thus greatly increasing the interest in the simultaneous determination of AA and DHAA in food products (Nováková et al., 2008; Mazurek & Jamroz, 2015; Spínola et al., 2014). However, as another major limitation of the electrochemical measurement can be seen in the fact that, in principle, DHAA cannot be directly determined. In HPLC analysis, tris[2-*carboxyethyl*]phosphine hydrochloride (TCEP) has been proposed as reducing agent to convert DHAA in AA in acidic conditions (Lykkesfeldt, 2000). Therefore, the electrochemical evaluation of the DHAA content in a milk sample, *via* its chemical reduction to AA by using TCEP, has been assessed.

Table 1 reports the vitamin C content detected from two aliquots (5 mL each) of milk samples, one of them added by TCEP, and then treated according to the procedure described in the Experimental section. The same table reports also the vitamin C content, detected on other two aliquots, 10 days aged, of the same milk samples, one of them treated with TCEP.

As it can be noticed from the values reported in Table 1, the TCEP-based procedure results in a promising protocol for the electrochemical determination of the total vitamin C content (AA + DHAA) in food samples, as well as to evaluate, by difference, the DHAA content. Further research will be able to identify the most suited experimental conditions to establish the analytical procedure for total vitamin C content determination on real samples.

4. Conclusions

Commercial foods and formulae for infants and young children are typically added by vitamin C, for granting the daily nutritional labeled intake and reduce the risk of scurvy. Thus, level monitoring of such a vitamin during food production and storage is a crucial concern among manufactures and consumers, and it requires the use of rapid screening methods for checking the vitamin C nutritional quality content.

Here, a novel nanostructured platform based on RGO flakes, surface decorated by colloidal Au NPs, has been tested and validated, as a direct and rapid (around 10 min considering the sample treatment) analytical method for quantifying vitamin C, by amperometry, in various fortified milk samples and infant formulae.

The novel nanostructured sensor platform exhibits a LOD lower than other graphene/Au NPs electrode modifiers reported in literature, and lower than that of a routine enzymatic-based spectrophotometric method. In particular, it shows a good linear response over the 50–500 μM concentration range with a LOD of 17 μM and a LOQ of 57 μM, with a %RSD of 8% (n = 5), when analyzing cow's milk samples. Some crucial advantages, such as low cost, easy sample preparation, fast response and reproducibility, as well as disposability of the sensor after usage, encourage its use in quality control laboratories, as alternative to routine enzymatic-based spectrophotometric methods for determining vitamin C in complex food matrices. The developed method is suited for the vitamin C determination in foods in which it is naturally present, especially in fruits and vegetables, and in the foods in which it is used as a nutritional food additive, stabilizer and as an antioxidant.

Finally, application of the proposed method can be envisaged in the determination of other species, and hence, it can find diverse applications in food chemistry and food manufacturer procedures.

Table 1
Detected vitamin C content of milk samples, as bare and treated with TCEP, before and after 10 days of ageing.

Sample	Vitamin C content (mg/100 mL)
Bare milk sample	14 ± 1
TCEP added milk sample	16 ± 1
Aged bare milk sample	6.0 ± 0.8
TCEP added aged milk sample	17 ± 2

Uncited references

Chen et al. (2002).

CRediT authorship contribution statement

Francesca Bettazzi: Investigation, Methodology. **Chiara Ingrosso:** Investigation, Conceptualization. **Patrick Severin Sfragano:** Investigation. **Valentina Pifferi:** Investigation. **Luigi Falciola:** Supervision. **M. Lucia Curri:** Supervision, Conceptualization. **Ilaria Palchetti:** Methodology, Writing - original draft, Supervision, Project administration.

Declaration of Competing Interest

The authors declare that they have no known competing financial interests or personal relationships that could have appeared to influence the work reported in this paper.

Acknowledgements

I.P. and F.B. acknowledege Mr M. Paolieri for helping in performing analysis of vitamin mix. Safe-water project (ERA-NET COFUND "Photonicsensing", GA no. 688735), for financial support (F.B. fellowship). Fondazione CR Firenze ID 2018.0944 for financial support (F.B. and P.S. fellowship).

Appendix A. Supplementary data

Supplementary data to this article can be found online at https://doi.org/10.1016/j.foodchem.2020.128692.

References

(EFSA), E. F. S. A. (2014). Scientific Opinion on the essential composition of infant and follow-on formulae. Https://Efsa.Onlinelibrary.Wiley.Com/Doi/Pdf/10.2903/j.Efsa.2014.3760.

Bettazzi, F., Palchetti, I., Sisalli, S., & Mascini, M. (2006). A disposable electrochemical sensor for vanillin detection. Analytica Chimica Acta, 555(1). doi:10.1016/j.aca.2005.08.069.

Bettazzi, F., Enayati, L., Sánchez, I.C., Motaghed, R., Mascini, M., & Palchetti, I. (2013). Electrochemical bioassay for the detection of TNF-α using magnetic

beads and disposable screen-printed array of electrodes. Bioanalysis, 5(1), 11–19. doi:10.4155/bio.12.293.
Bettazzi, F., Laschi, S., Voccia, D., Gellini, C., Pietraperzia, G., Falciola, L., … Palchetti, I. (2018). Ascorbic acid-sensitized Au nanorods-functionalized nanostructured TiO_2 transparent electrodes for photoelectrochemical genosensing. Electrochimica Acta, 276, 389–398. doi:10.1016/j.electacta.2018.04.146.
Bonanni, A., Ambrosi, A., & Pumera, M. (2012). On Oxygen-Containing Groups in Chemically Modified Graphenes. *Chemistry – A*. European Journal, 18(15), 4541–4548. doi:10.1002/chem.201104003.
Brunetti, B., & Desimoni, E. (2014). Voltammetric determination of vitamin B6 in food samples and dietary supplements. Journal of Food Composition and Analysis, 33(2), 155–160. doi:10.1016/j.jfca.2013.12.008.
Chebrolu, K.K., Jayaprakasha, G.K., Yoo, K.S., Jifon, J.L., & Patil, B.S. (2012). An improved sample preparation method for quantification of ascorbic acid and dehydroascorbic acid by HPLC. LWT - Food Science and Technology, 47(2), 443–449. doi:10.1016/j.lwt.2012.02.004.
Chen, J., Gorton, L., & Åkesson, B. (2002). Electrochemical studies on antioxidants in bovine milk. Analytica Chimica Acta, 474(1), 137–146. doi:10.1016/S0003-2670(02)01004-8.
Compton, R. G., & Banks, C. E. (2010). Understanding Voltammetry. IMPERIAL COLLEGE PRESS. 10.1142/p726
da Silva, T.L., Aguiar-Oliveira, E., Mazalli, M.R., Kamimura, E.S., & Maldonado, R.R. (2017). Comparison between titrimetric and spectrophotometric methods for quantification of vitamin C. Food Chemistry, 224, 92–96. doi:10.1016/j.foodchem.2016.12.052.
Danielczuk, J., Pietrzykowski, R., & Zieliński, W. (2004). Comparative study of the enzymatic method for determination of vitamin c with routine methods according to ISO. Polish Journal of Food and Nutrition Sciences, 54(1), 41–46.
EFSA Panel on Dietetic Products, N. and A. (NDA). (2013). Scientific Opinion on nutrient requirements and dietary intakes of infants and young children in the European Union. EFSA Journal.
European commission. (2006). Regulation (EC) No 1925/2006 of the European Parliament and of the Council of 20 December 2006 on the addition of vitamins and minerals and of certain other substances to foods. OJ L 404.
Falat, L., & Cheng, H.-Y. (1983). Electrocatalysis of ascorbate and NASH at a surface modified graphite-epoxy electrode. Journal of Electroanalytical Chemistry and Interfacial Electrochemistry, 157(2), 393–397. doi:10.1016/S0022-0728(83)80366-0.
Gazdik, Z., Zitka, O., Petrlova, J., Adam, V., Zehnalek, J., Horna, A., … Kizek, R. (2008). Determination of Vitamin C (Ascorbic Acid) Using High Performance Liquid Chromatography Coupled with Electrochemical Detection. Sensors, 8, 7097–7112.
Ghanbari, K., & Hajian, A. (2017). Electrochemical characterization of Au/ZnO/PPy/RGO nanocomposite and its application for simultaneous determination of ascorbic acid, epinephrine, and uric acid. Journal of Electroanalytical Chemistry, 801, 466–479. doi:10.1016/j.jelechem.2017.07.024.
Goncalves, G., Marques, P.A.A.P., Granadeiro, C.M., Nogueira, H.I.S., Singh, M.K., & Grácio, J. (2009). Surface Modification of Graphene Nanosheets with Gold Nanoparticles: The Role of Oxygen Moieties at Graphene Surface on Gold Nucleation and Growth. Chemistry of Materials, 21(20), 4796–4802. doi:10.1021/cm901052s.
Ingrosso, C., Bianco, G.V., Pifferi, V., Guffanti, P., Petronella, F., Comparelli, R., … Bruno, G. (2017). Enhanced photoactivity and conductivity in transparent TiO2 nanocrystals/graphene hybrid anodes. Journal of Materials Chemistry A, 5(19), 9307–9315. doi:10.1039/C7TA01425B.
Ingrosso, C., Corricelli, M., Disha, A., Fanizza, E., Bianco, G.V., Depalo, N., … Curri, M.L. (2019). Solvent dispersible nanocomposite based on Reduced Graphene Oxide in situ decorated with gold nanoparticles. Carbon, 152, 777–787. doi:10.1016/j.carbon.2019.06.070.
Ingrosso, C., Corricelli, M., Bettazzi, F., Konstantinidou, E., Bianco, G.V., Depalo, N., … Palchetti, I. (2019). Au nanoparticle in situ decorated RGO nanocomposites for highly sensitive electrochemical genosensors. Journal of Materials Chemistry B, 7(5), 768–777. doi:10.1039/C8TB02514B.
Klingler, R.J., & Kochi, J.K. (1980). Heterogeneous rates of electron transfer. Application of cyclic voltammetric techniques to irreversible electrochemical processes. Journal of the American Chemical Society, 102(14), 4790–4798. doi:10.1021/ja00534a036.
Laschi, S., Palchetti, I., Marrazza, G., & Mascini, M. (2006). Development of disposable low density screen-printed electrode arrays for simultaneous electrochemical measurements of the hybridisation reaction. Journal of Electroanalytical Chemistry, 593(1–2). doi:10.1016/j.jelechem.2006.04.015.
Lermo, A., Fabiano, S., Hernández, S., Galve, R., Marco, M.-P., Alegret, S., & Pividori, M.I. (2009). Immunoassay for folic acid detection in vitamin-fortified milk based on electrochemical magneto sensors. Biosensors and Bioelectronics, 24(7), 2057–2063. doi:10.1016/j.bios.2008.10.020.
Liu, G., Wang, Y.M., & Sun, D.M. (2016). Simultaneous determination of vitamins B2, B6 and C using silver-doped poly(L-arginine)-modified glassy carbon electrode. Journal of Analytical Chemistry, 71(1), 102–109. doi:10.1134/S1061934815120114.
Llorent-Martínez, E.J., García-Reyes, J.F., Ortega-Barrales, P., & Molina-Díaz, A. (2006). A multicommuted fluorescence-based sensing system for simultaneous determination of Vitamins B2 and B6. Analytica Chimica Acta, 555(1), 128–133. doi:10.1016/j.aca.2005.08.054.
Lykkesfeldt, J. (2000). Determination of Ascorbic Acid and Dehydroascorbic Acid in Biological Samples by High-Performance Liquid Chromatography Using Subtraction Methods: Reliable Reduction with Tris[2-carboxyethyl]phosphine Hydrochloride. Analytical Biochemistry, 282(1), 89–93. doi:10.1006/abio.2000.4592.
Mazurek, A., & Jamroz, J. (2015). Precision of dehydroascorbic acid quantitation with the use of the subtraction method – Validation of HPLC–DAD method for determination of total vitamin C in food. Food Chemistry, 173, 543–550. doi:10.1016/j.foodchem.2014.10.065.
National Academies of Sciences Engineering Medicine. (n.d.). Recommended Dietary Allowance and Adequate Intake Values, Vitamins and Elements,. http://Nationalacademies.Org/Hmd/~/Media/Files/Activity%20Files/Nutrition/DRI-Tables/2_%20RDA%20and%20AI%20Values_Vitamin%20and%20Elements.Pdf?La=en.
Nicholson, R.S., & Shain, I. (1964). Theory of Stationary Electrode Polarography. Single Scan and Cyclic Methods Applied to Reversible, Irreversible, and Kinetic Systems. Analytical Chemistry, 36(4), 706–723. doi:10.1021/ac60210a007.
Nováková, L., Solich, P., & Solichová, D. (2008). HPLC methods for simultaneous determination of ascorbic and dehydroascorbic acids. TrAC Trends in Analytical Chemistry, 27(10), 942–958.
Pisoschi, A.M., Pop, A., Serban, A.I., & Fafaneata, C. (2014). Electrochemical methods for ascorbic acid determination. Electrochimica Acta, 121, 443–460. doi:10.1016/j.electacta.2013.12.127.
Puangjan, A., Chaiyasith, S., Taweeporngitgul, W., & Keawtep, J. (2017). Application of functionalized multi-walled carbon nanotubes supporting cuprous oxide and silver oxide composite catalyst on copper substrate for simultaneous detection of vitamin B2, vitamin B6 and ascorbic acid. Materials Science and Engineering: C, 76, 383–397. doi:10.1016/j.msec.2017.03.040.
Romeu-Nadal, M., Morera-Pons, S., Castellote, A.I., & López-Sabater, M.C. (2006). Rapid high-performance liquid chromatographic method for Vitamin C determination in human milk versus an enzymatic method. Journal of Chromatography B, 830(1), 41–46. doi:10.1016/j.jchromb.2005.10.018.
Rueda, M., Aldaz, A., & Sanchez-Burgos, F. (1978). Oxidation of L-ascorbic acid on a gold electrode. Electrochimica Acta, 23(5), 419–424. doi:10.1016/0013-4686(78)87040-6.
Silva, M.A., Albuquerque, T.G., Oliveira, M.B.P.P., & Costa, H.S. (2018). Vitamin C evaluation in foods for infants and young children by a rapid and accurate analytical method. Food Chemistry, 267, 83–90. doi:10.1016/j.foodchem.2017.11.046.
Spínola, V., Llorent-Martínez, E.J., & Castilho, P.C. (2014). Determination of vitamin C in foods: Current state of method validation. Journal of Chromatography A, 1369, 2–17. doi:10.1016/j.chroma.2014.09.087.
Tian, X., Cheng, C., Yuan, H., Du, J., Xiao, D., Xie, S., & Choi, M.M.F. (2012). Simultaneous determination of l-ascorbic acid, dopamine and uric acid with gold nanoparticles–β-cyclodextrin–graphene-modified electrode by square wave voltammetry. Talanta, 93, 79–85. doi:10.1016/j.talanta.2012.01.047.
Tiwari, I., Gupta, M., Pandey, C.M., & Mishra, V. (2015). Gold nanoparticle decorated graphene sheet-polypyrrole based nanocomposite: Its synthesis, characterization and genosensing application. Dalton Transactions, 44(35), 15557–15566. doi:10.1039/C5DT01193K.
Turcheniuk, K., Boukherroub, R., & Szunerits, S. (2015). Gold-graphene nanocomposites for sensing and biomedical applications. J. Mater. Chem. B.. doi:10.1039/C5TB00511F.
Wang, C., Du, J., Wang, H., Zou, C., Jiang, F., Yang, P., & Du, Y. (2014). A facile electrochemical sensor based on reduced graphene oxide and Au nanoplates modified glassy carbon electrode for simultaneous detection of ascorbic acid, dopamine and uric acid. Sensors and Actuators B: Chemical, 204, 302–309. doi:10.1016/j.snb.2014.07.077.
Zhao, Y., Zhou, J., Jia, Z., Huo, D., Liu, Q., Zhong, D., … Hou, C. (2019). In-situ growth of gold nanoparticles on a 3D-network consisting of a MoS2/rGO nanocomposite for simultaneous voltammetric determination of ascorbic acid, dopamine and uric acid. Microchimica Acta, 186(2), 92. doi:10.1007/s00604-018-3222-7.
Zhu, Q., Bao, J., Huo, D., Yang, M., Hou, C., Guo, J., … Ma, Y. (2017). 3D Graphene hydrogel – gold nanoparticles nanocomposite modified glassy carbon electrode for the simultaneous determination of ascorbic acid, dopamine and uric acid. Sensors and Actuators B: Chemical, 238, 1316–1323. doi:10.1016/j.snb.2016.09.116.